computation

MDPI

Article

Extension of Cubic B-Spline for Solving the Time-Fractional Allen–Cahn Equation in the Context of Mathematical Physics

Mubeen Fatima [1], Ravi P. Agarwal [2], Muhammad Abbas [1], Pshtiwan Othman Mohammed [3,4,*], Madiha Shafiq [1] and Nejmeddine Chorfi [5]

[1] Department of Mathematics, University of Sargodha, Sargodha 40100, Pakistan; muhammad.abbas@uos.edu.pk (M.A.)
[2] Department of Mathematics, Texas A & M University-Kingsville, Kingsville, TX 78363, USA; ravi.agarwal@tamuk.edu
[3] Department of Mathematics, College of Education, University of Sulaimani, Sulaymaniyah 46001, Iraq
[4] Research and Development Center, University of Sulaimani, Sulaymaniyah 46001, Iraq
[5] Department of Mathematics, College of Science, King Saud University, P.O. Box 2455, Riyadh 11451, Saudi Arabia; nchorfi@ksu.edu.sa
* Correspondence: pshtiwansangawi@gmail.com

Abstract: A B-spline is defined by the degree and quantity of knots, and it is observed to provide a higher level of flexibility in curve and surface layout. The extended cubic B-spline (ExCBS) functions with new approximation for second derivative and finite difference technique are incorporated in this study to solve the time-fractional Allen–Cahn equation (TFACE). Initially, Caputo's formula is used to discretize the time-fractional derivative, while a new ExCBS is used for the spatial derivative's discretization. Convergence analysis is carried out and the stability of the proposed method is also analyzed. The scheme's applicability and feasibility are demonstrated through numerical analysis.

Keywords: finite difference; Caputo fractional derivative; new ExCBS functions; time-fractional Allen–Cahn equation; stability and convergence

MSC: 41A15; 65D07; 35R11; 26A33; 65M22

Citation: Fatima, M.; Agarwal, R.P.; Abbas, M.; Mohammed, P.O.; Shafiq, M.; Chorfi, N. Extension of Cubic B-Spline for Solving the Time-Fractional Allen–Cahn Equation in the Context of Mathematical Physics. *Computation* **2024**, *12*, 51. https://doi.org/10.3390/computation12030051

Academic Editors: Endre Kovács, Denis Butusov and Valerii Ostrovskii

Received: 22 January 2024
Revised: 2 March 2024
Accepted: 3 March 2024
Published: 5 March 2024

1. Introduction

The term spline describes the various features used in applications that require data interpolation and smoothing. The B-spline functions are highly localized. That is, the non-zero values occur only at the small intervals, and the B-spline coefficient contains the overall behaviour of the original function. These functions in general provide the most flexible way to define curves in computer graphics. A B-spline contains sections of polynomial curves connected at places called nodes. A linear combination of B-splines of a particular degree can be used to express any spline function of that degree. Over the past few years, numerical equations have become a powerful and useful mathematical tool for studying many phenomena in science and engineering. The study of differential equations is multidisciplinary and is applied in many ways including control, flexibility, circuit systems, heat transfer, quantum mechanics, fluid mechanics, biomathematics, biomedicine systems, traffic turbulence, complex systems and pollution control etc [1–4]. The ACE is a simple model of a nonlinear reaction–diffusion process. It is widely used to model the behavior of the interface at a given time, e.g., alloy phase separation. There are many applications for nonlinear evaluation equations in engineering, physics, chemistry and biology [5–7].

The fractional derivative can better represent several phenomena than the integer order derivative. The Caputo derivative is the most appropriate fractional operator to use when modeling real-world problems. For solving fractional ordinary differential equations,

integral equations and fractional partial differential equations (FPDEs), many techniques are presented in the literature. The first integral scheme was used by Lu [8] to obtain the exact solution of the time-fractional differential equation. He and Wu [9] discussed the Exp-function technique to find the independent solutions of different non-linear wave equations. The exact solution for space- and time-fractional derivatives foam drainage and non-linear KdV equations using a better (G'/G) expansion function method was presented by Gepreel and Omran [10]. The fractional variable method was tested by Liu and Chen [11].

Bulut et al. [12] discussed the modified trial equation technique. A fractional sub-equation scheme for FPDE was proposed by Zheng and Wen [13]. The simplest equation method for solving time FPDE was discussed by Taghizadeh et al. [14]. For solving fractional non-linear problems, the Tanh-fractional method was used by Sahoo and Ray [15]. Tariq and Akram [16] developed an improved Tanh approach for solving non-linear equation that arises in mathematical physics, especially ACE. Types of Allen–Cahn and Cahn–Hilliard PDE models of the critical category were discussed by Prüss and Wilke [17]. Appadu et al. [18] compared explicit and implicit one-level techniques with multilevel finite volume methods. For biofilm formation, Tijani and Appadu [19] constructed a mathematical model on medical implant with finite difference method. Allen and Cahn [20] introduced the microscopic diffusion theory of the movement of curved boundary opposes solid crystal. Some authors also discussed various applications such as the interaction between two fixed fluids, the vesicle membrane and the nucleation solids [21–23]. Li et al. [24] presented finite element scheme for FPDEs.

In this paper, a fully implicit finite difference scheme is formulated to obtain the numerical solution of TFACE based on new ExCBS. For time discretization, Caputo's formula is used and a new ExCBS is utilized to discretize the spatial derivative. The TFACE is given as [5]:

$$\frac{\partial^{\gamma}}{\partial t^{\gamma}}q(p,t) - \frac{\partial^{2}}{\partial p^{2}}q(p,t) + (q(p,t))^{3} - q(p,t) = \nu(p,t), \quad p \in [a,b], \quad t \in [0,T], \tag{1}$$

with initial condition (IC):

$$q(p,0) = \varphi(p) \tag{2}$$

and the boundary conditions (BCs):

$$q(a,t) = \Psi_1(t), \; q(b,t) = \Psi_2(t), \tag{3}$$

where $\gamma \in (0,1)$ and $\nu(p,t)$ is the source term. Ψ and φ are smooth and continuous functions with first order derivatives.

Domain coarsening in a sub-diffusive ACE in terms of the Seki–Lindenberg sub diffusion reaction model was studied by Hamed and Nepomnyashchy [25]. Different types of specific solutions from first integral, (G'/G) expansion and the exp-function methods were explored by Güner et al. [26]. Zhai et al. [27] solved the fractional non-local Allen–Cahn model very quickly using explicit operator splitting spectral method. Akagi et al. [28] proved that weak solutions of ACE, fractional porous medium and fractional-diffusion fast equation exist and are unique. The Crank–Nicolson approach and second order central difference scheme for spatial and temporal fragmentation were used by Hou et al. [29]. Li et al. [30] introduced a TFAC phase field model that illustrates the transportation of a liquid mixture of two unmixable liquid phases. New exact and explicit solutions for TFAC and Cahn–Hilliard equations with fractional derivatives were presented by Hosseini et al. [31]. Sakar et al. [32] developed a novel iterative scheme based on reproducing ACE kernel method with Caputo derivative. Liu et al. [33] investigated the time-fractional models of Allen–Cahn and Cahn–Hilliard using Fourier spectral and finite difference methods. To solve the non-linear space-fractional ACE numerically, a fast time-based two-mesh finite element technique was developed by Yin et al. [34]. To find the computational solutions of Allen–Cahn and damped Burger equations the homotopy analysis technique was used by Esen et al. [35].

Inc et al. [36] reduced the TFAC and time-fractional KG into non-linear ordinary differential equations of fractional order and solved these ordinary differential equations by employing an explicit power series algorithm. Shafiq et al. [37–39] proposed numerical techniques for time-fractional diffusion, Burgers' and advection diffusion equations with fractional derivatives using CBS functions. Khalid et al. [40] proposed a third-degree algorithm optimized for ExCBS functions to solve the time-fractional diffusion wave equation. To find the computational results of fourth-order fractional boundary value problems (BVPs), the reproducing kernel Hilbert space scheme was used by Akgül and Karatas Akgül [41]. A computational method using the conformable fractional derivative was proposed by Tayebi et al. [42] with CBS functions. Appadu and Kelil [43] proposed computational solutions of time-fractional Korteweg de Vries model utilizing finite difference techniques with fractional derivative. Atangana and Gómez-Aguilar [44] used the definition of Riemann-Liouville to find the numerical approximation of fractional operators from power-law kernel. Akgül [45] utilized the Mittag–Leffler operator to find the solutions of non-linear and linear FPDEs. Mittal and Jain [46] established a collocation scheme to solve the convection–diffusion equation utilizing redefined CBS functions.

Rashidinia and Sharifi [47] developed a scheme for hyperbolic telegraph equation based on ExCBS and this approach reduced the size of computational work. Liu et al. [48] proposed implicit difference and explicit difference techniques to find the computational solution of time-fractional advection dispersion problem. To achieve the numerical solutions of nonlinear PDE, a PECE-type based algorithm was used by Diethelm and Freed [49]. To obtain the solution of fractional diffusion equation CBS collocation technique was used by Sayevand et al. [50]. Akram and Tariq [51] established a numerical approach using quintic spline algorithm to acquire the results of fractional BVPs. Tasbozan et al. [52] implemented an approximate method based on CBS function to attain the solution of fractional diffusion equation. Boyce et al. [53] provided a numerical solution for elementary differential equation and BVPs. Kadalbajoo and Arora [54] established a B-spline collocation methodology that solves singular-perturbed equation using artificial viscosity. Convergence of odd degree equation and error bounds for spline interpolation presented in [55–57].

The presented work is inspired by progressive advances in TFACE numerical analysis. In this study, we developed and applied a new B-spline based scheme to obtain solution for TFACE. The proposed strategy uses Caputo's formula to discretize time-fractional derivative and to discretize spatial derivative new ExCBS are used. Furthermore, the convergence and stability of proposed strategy is accomplished. To the best of author's knowledge, the presented method is new and has not been reported before in the literature.

This paper is classified as follows: In Section 2, ExCBS functions and a new approximation of second derivative for ExCBS are presented. Time discretization of Caputo-fractional derivative and fully implicit finite difference scheme are briefly described in Section 3. In Section 4, initial state η^0 is expressed. In Section 5, the stability analysis is expounded. Convergence analysis of the proposed technique is presented in Section 6. In Section 7, two numerical examples are included for proposed method.

2. Extended Cubic B-Spline Functions

ExCBS is the extension of CBS with an additional free parameter ϱ. The free parameter is introduced in basis functions to allow changes to the generated curves.

The basis function of ExCBS with four degrees is defined as follows [40]:

$$C_j(p,\varrho)=\frac{1}{24h^4}\begin{cases}4h(1-\varrho)(p-p_j)^3+3\varrho(p-p_j)^4, & p\in[p_j,p_{j+1}),\\ (4-\varrho)h^4+12h^3(p-p_{j+1})+6h^2(2+\varrho)(p-p_{j+1})^2 & \\ -12h(p-p_{j+1})^3-3\varrho(p-p_{j+1})^4, & p\in[p_{j+1},p_{j+2}),\\ (4-\varrho)h^4+12h^3(p_{j+3}-p)+6h^2(2+\varrho)(p_{j+3}-p)^2 & \\ -12h(p_{j+3}-p)^3-3\varrho(p_{j+3}-p)^4, & p\in[p_{j+2},p_{j+3}),\\ 4h(1-\varrho)(p_{j+4}-p)^3+3\varrho(p_{j+4}-p)^4, & p\in[p_{j+3},p_{j+4}),\\ 0, & \text{otherwise},\end{cases} \tag{4}$$

where p is the variable and $\varrho\in R$. For $-8\le\varrho\le 1$, the ExCBS functions possess the various properties of B-spline, such as the convex hull property, symmetry and geometric invariance. If we substitute $\varrho=0$, the basis function of extended spline will reduce to CBS function. Now, consider the ExCBS approximation for $q(p,t)$ to be $Q(p,t)$ as

$$Q(p,t)=\sum_{k=-1}^{n+1}\eta_k^m(t)C_k(p,\varrho), \tag{5}$$

where $\eta_k^m(t)$ are the control points which are computed at each time level and $C_k(p,\varrho)$ are the ExCBS functions. Due to the local support property of basis function, that is $C_k(p,\varrho)$ are non-zero in $[p_j,p_{j+4})$, it contains only three non-zero basis functions, namely $C_{k-1}(p,\varrho)$, $C_k(p,\varrho)$ and $C_{k+1}(p,\varrho)$ for the evaluation at each p_j.

The coefficients of ExCBS functions and their derivatives at knots p_j are:

$$C(p_j,\varrho)=\begin{cases}\frac{8+\varrho}{12}, & \text{if } k-j=0,\\ \frac{4-\varrho}{24}, & \text{if } k-j=\pm1,\\ 0, & \text{otherwise},\end{cases} \tag{6}$$

$$C'(p_j,\varrho)=\begin{cases}0, & \text{if } k-j=0,\\ \pm\frac{1}{2h}, & \text{if } k-j=\pm1,\\ 0, & \text{otherwise},\end{cases} \tag{7}$$

$$C''(p_j,\varrho)=\begin{cases}-\frac{2+\varrho}{h^2}, & \text{if } k-j=0,\\ \frac{2+\varrho}{h^2}, & \text{if } k-j=\pm1,\\ 0, & \text{otherwise}.\end{cases} \tag{8}$$

Formulation of New Approximation for $Q''(p,t)$

To find new ExCBS functions $Q''(p,t)$ for second derivative $q''(p_j)$ [58]:

$$C_0=\frac{1}{24h^2}\big(2(14-\varrho)\eta_{-1}+3(3\varrho-22)\eta_0+8(7-2\varrho)\eta_1+14(\varrho-2)\eta_2+6(2-\varrho)\eta_3+(\varrho-2)\eta_4\big). \tag{9}$$

$$C_j=\frac{1}{24h^2}\big((2-\varrho)\eta_{j-2}+4(4+\varrho)\eta_{j-1}-6(6+\varrho)\eta_j+4(4+\varrho)\eta_{j+1}+(2-\varrho)\eta_{j+2}\big). \tag{10}$$

$$C_n=\frac{1}{24h^2}\big((\varrho-2)\eta_{n-4}+6(2-\varrho)\eta_{n-3}+14(\varrho-2)\eta_{n-2}+8(7-2\varrho)\eta_{n-1}+3(3\varrho-22)\eta_n+2(14-\varrho)\eta_{n+1}\big). \tag{11}$$

3. Description of Scheme

3.1. Temporal Discretization

Consider the time interval $[0, T]$ by taking the knots $0 = t_0 < t_1 < \ldots < t_Z = T$, where $t_m = m \triangle t$ and $m = 0, 1, \ldots, Z$, subdivided into Z equal subintervals of size $\triangle t = \frac{T}{Z}$. We discretize the time derivative of the Allen–Cahn Equation (1) at $t = t_{m+1}$ as:

$$\begin{aligned} \frac{\partial^\gamma}{\partial t^\gamma} q(p, t_{m+1}) &= \frac{1}{\Gamma(1-\gamma)} \int_0^{t_{m+1}} \frac{\partial}{\partial \tau} q(p, \tau) \frac{1}{(t_{m+1} - \tau)^\gamma} d\tau, \qquad 0 < \varrho < 1, \\ &= \frac{1}{\Gamma(1-\gamma)} \sum_{s=0}^{m} \int_{t_s}^{t_{s+1}} \frac{\partial}{\partial \tau} q(p, \tau) \frac{1}{(t_{m+1} - \tau)^\gamma} d\tau. \end{aligned} \tag{12}$$

Using forward difference formulation, Equation (12) becomes

$$\begin{aligned} \frac{\partial^\gamma}{\partial t^\gamma} q(p, t_{m+1}) &= \frac{1}{\Gamma(1-\gamma)} \sum_{s=0}^{m} \frac{q(p, t_{s+1}) - q(p, t_s)}{\triangle t} \int_{t_s}^{t_{s+1}} \frac{1}{(t_{m+1} - \tau)^\gamma} d\tau + \varrho_{\triangle t}^{m+1} \\ &= \frac{1}{\Gamma(1-\gamma)} \sum_{s=0}^{m} \frac{q(p, t_{s+1}) - q(p, t_s)}{\triangle t} \int_{t_{m-s}}^{t_{m-s+1}} \frac{1}{(\rho)^\gamma} d\rho + \varrho_{\triangle t}^{m+1} \\ &= \frac{1}{\Gamma(1-\gamma)} \sum_{s=0}^{m} \frac{q(p, t_{m-s+1}) - q(p, t_{m-s})}{\triangle t} \int_{t_s}^{t_{s+1}} \frac{1}{(\rho)^\gamma} d\rho + \varrho_{\triangle t}^{m+1} \\ &= \frac{1}{\Gamma(2-\gamma)} \sum_{s=0}^{m} \frac{q(p, t_{m-s+1}) - q(p, t_{m-s})}{(\triangle t)^\gamma} [(\ell+1)^{1-\gamma} - (\ell)^{1-\gamma}] + \varrho_{\triangle t}^{m+1} \end{aligned}$$

$$\frac{\partial^\gamma}{\partial t^\gamma} q(p, t_{m+1}) = \frac{1}{\Gamma(2-\gamma)} \sum_{s=0}^{m} \xi_s \frac{q(p, t_{m-s+1}) - q(p, t_{m-s})}{(\triangle t)^\gamma} + \varrho_{\triangle t}^{m+1}, \tag{13}$$

where $\rho = t_{m+1} - \tau$, $\xi_s = (\ell+1)^{1-\gamma} - (\ell)^{1-\gamma}$ and the truncation error $\varrho_{\triangle t}^{m+1}$ is bounded as:

$$| \varrho_{\triangle t}^{m+1} | \leq \delta (\triangle t)^{2-\gamma}, \tag{14}$$

where δ is the finite constant.

Lemma 1. *The coefficients ξ_s satisfy the following characteristics*

- $\xi_s > 0$ *and* $\xi_0 = 1$, $s = 1, 2, \ldots, m$,
- $\xi_0 > \xi_1 > \xi_2 > \ldots > \xi_s$, $\xi_s \to 0$ *as* $s \to \infty$,
- $\sum_{s=0}^{m} (\xi_s - \xi_{s+1}) + \xi_{m+1} = (1 - \xi_1) + \sum_{s=1}^{m-1} (\xi_s - \xi_{s+1}) + \xi_m = 1$.

3.2. Fully Implicit Scheme

Here, a fully implicit scheme is applied to discretize the time derivative. This scheme is linear that has an accuracy of second order in time.

Let $q_j^m = q(p_j, t^m)$, $(q(p,t))^3 = F(q(p,t))$ and substitute $\nu(p, t_{m+1}) - F(q(p,t)) = g^{m+1}$. $\eta_j^m = \eta_j(t^m)$ for $j = 0, 1, 2, \ldots, n$ and $m = 0, 1, \ldots, Z$.

For $j = 1, 2, \ldots, n-1$, substitute Equations (6) and (10) in Equation (1), we have

$$\begin{aligned} &\frac{1}{\Gamma(2-\gamma)(\triangle t)^\gamma} \sum_{s=0}^{m} \xi_s \left[\frac{(4-\varrho)}{24} \eta_{j-1}^{m-s+1} + \frac{(8+\varrho)}{12} \eta_j^{m-s+1} + \frac{(4-\varrho)}{24} \eta_{j+1}^{m-s+1} - \frac{(4-\varrho)}{24} \eta_{j-1}^{m-s} \right. \\ &\left. - \frac{(8+\varrho)}{12} \eta_j^{m-s} - \frac{(4-\varrho)}{24} \eta_{j+1}^{m-s} \right] - \frac{1}{24h^2} \left[(2-\varrho) \eta_{j-2}^{m+1} + 4(4+\varrho) \eta_{j-1}^{m+1} - 6(6+\varrho) \eta_j^{m+1} \right. \\ &\left. + 4(4+\varrho) \eta_{j+1}^{m+1} + (2-\varrho) \eta_{j+2}^{m+1} \right] - \left[\frac{(4-\varrho)}{24} \eta_{j-1}^{m+1} + \frac{(8+\varrho)}{12} \eta_j^{m+1} + \frac{(4-\varrho)}{24} \eta_{j+1}^{m+1} \right] = g^{m+1}. \end{aligned} \tag{15}$$

Simplification of the above equation yields

$$\begin{aligned}[rv_1 - l_8 - v_1]\eta_{j-1}^{m+1} + [rv_2 + l_9 - v_2]\eta_j^{m+1} + [rv_1 - l_8 - v_1]\eta_{j+1}^{m+1} - l_7\eta_{j-2}^{m+1} - l_7\eta_{j+2}^{m+1} \\ = r[v_1\eta_{j-1}^m + v_2\eta_j^m + v_1\eta_{j+1}^m] - r\sum_{s=1}^{m}\xi_s[v_1(\eta_{j-1}^{m-s+1} - \eta_{j-1}^{m-s}) + v_2(\eta_j^{m-s+1} - \eta_j^{m-s}) \\ + v_1(\eta_{j+1}^{m-s+1} - \eta_{j+1}^{m-s})] + g^{m+1}.\end{aligned} \tag{16}$$

For $j = 0$, substitute Equations (6) and (9) in Equation (1), we obtain

$$\begin{aligned}[rv_1 - l_1 - v_1]\eta_{-1}^{m+1} + [rv_2 - l_2 - v_2]\eta_0^{m+1} + [rv_1 - l_3 - v_1]\eta_1^{m+1} - l_4\eta_2^{m+1} - l_5\eta_3^{m+1} \\ - l_6\eta_4^{m+1} = r[v_1\eta_{-1}^m + v_2\eta_0^m + v_1\eta_1^m] - r\sum_{s=1}^{m}\xi_s[v_1(\eta_{-1}^{m-s+1} - \eta_{-1}^{m-s}) + v_2(\eta_0^{m-s+1} - \eta_0^{m-s}) \\ + v_1(\eta_1^{m-s+1} - \eta_1^{m-s})] + g^{m+1}.\end{aligned} \tag{17}$$

For $j = n$, substitute Equations (6) and (11) in Equation (1), we have

$$\begin{aligned}[rv_1 - l_3 - v_1]\eta_{n-1}^{m+1} + [rv_2 - l_2 - v_2]\eta_n^{m+1} + [rv_1 - l_1 - v_1]\eta_{n+1}^{m+1} - l_6\eta_{n-4}^{m+1} - l_5\eta_{n-3}^{m+1} \\ - l_4\eta_{n-2}^{m+1} = r[v_1\eta_{n-1}^m + v_2\eta_n^m + v_1\eta_{n+1}^m] - r\sum_{s=1}^{m}\xi_s[v_1(\eta_{n-1}^{m-s+1} - \eta_{n-1}^{m-s}) + v_2(\eta_n^{m-s+1} - \eta_n^{m-s}) \\ + v_1(\eta_{n+1}^{m-s+1} - \eta_{n+1}^{m-s})] + g^{m+1},\end{aligned} \tag{18}$$

where $v_1 = \frac{(4-\varrho)}{24}, v_2 = \frac{(8+\varrho)}{12}, v_3 = \frac{1}{2h}, l_1 = \frac{2(14-\varrho)}{24h^2}, l_2 = \frac{3(3\varrho-22)}{24h^2}, l_3 = \frac{8(7-2\varrho)}{24h^2}, l_4 = \frac{14(\varrho-2)}{24h^2}$, $l_5 = \frac{6(2-\varrho)}{24h^2}, l_6 = \frac{\varrho-2}{24h^2}, l_7 = \frac{2-\varrho}{24h^2}, l_8 = \frac{4(4+\varrho)}{24h^2}$ and $l_9 = \frac{6(6+\varrho)}{24h^2}$.

The above system contains $n+1$ linear equations in $n+3$ unknowns. To obtain a unique solution, two more equations are obtained from the BCs. Hence, a matrix system of dimension $(n+3) \times (n+3)$ is acquired:

$$A\eta^{m+1} = B(\xi_m\eta^0 + \sum_{s=0}^{m-1}(\xi_s - \xi_{s+1})\eta^{m-s}) + G, \tag{19}$$

where

$$A = \begin{bmatrix} v_1 & v_2 & v_1 & & & & & & & \\ y_1 & y_2 & y_3 & y_4 & y_5 & & & & & \\ & y_1 & y_2 & y_3 & y_4 & y_5 & & & & \\ & & & \ddots & \ddots & \ddots & & & & \\ & & & & y_1 & y_2 & y_3 & y_4 & y_5 & \\ & & & & & y_1 & y_2 & y_3 & y_4 & y_5 \\ & & & & & v_1 & v_2 & v_1 & & \end{bmatrix}, \quad B = \begin{bmatrix} 0 & 0 & 0 & & & & & & & \\ v_1 & v_2 & v_1 & & & & & & & \\ & v_1 & v_2 & v_1 & & & & & & \\ & & & \ddots & \ddots & \ddots & & & & \\ & & & & & & v_1 & v_2 & v_1 & \\ & & & & & & & v_1 & v_2 & v_1 \\ & & & & & & & 0 & 0 & 0 \end{bmatrix},$$

$$\eta^m = \begin{bmatrix} \eta_{-1}^m \\ \eta_0^m \\ \eta_1^m \\ \vdots \\ \eta_{n-1}^m \\ \eta_n^m \\ \eta_{n+1}^m \end{bmatrix} \text{ and } G = \begin{bmatrix} \Psi_1^{m+1} \\ g_0^{m+1} \\ g_1^{m+1} \\ \vdots \\ g_{n-1}^{m+1} \\ g_n^{m+1} \\ \Psi_2^{m+1} \end{bmatrix},$$

where $y_1 = rv_1 - l_8 - v_1, y_2 = rv_2 + l_9 - v_2, y_3 = rv_1 - l_8 - v_1$ and $y_4 = y_5 = -l_7$.

4. Initial State η^0

In this section, a suitable initial vector $\eta^0 = [\eta^0_{-1}, \eta^0_0, \ldots, \eta^0_{n+1}]^T$ from IC is constructed to start iteration. The IC together with its derivatives are given as follows:

$$(q_p)^0_j = \frac{d}{dp}(\varphi(p_j)), \quad j = 0, n$$

and

$$q^0_j = q(p_j, 0) = \sum_{j=1}^{n+1} \eta^0_j(0) C(p_j), \quad j = 0, 1, \ldots, n.$$

The above system is a linear algebraic system of order $(n+3) \times (n+3)$, its matrix representation is given as:

$$\acute{D}\eta^0 = H, \tag{20}$$

where

$$\acute{D} = \begin{bmatrix} v_3 & 0 & -v_3 & & & & & & \\ v_1 & v_2 & v_1 & & & & & & \\ & v_1 & v_2 & v_1 & & & & & \\ & & & \ddots & \ddots & \ddots & & & \\ & & & & & v_1 & v_2 & v_1 & \\ & & & & & & v_1 & v_2 & v_1 \\ & & & & & & v_3 & 0 & -v_3 \end{bmatrix} \text{ and } H = \begin{bmatrix} \varphi'_0 \\ \varphi_0 \\ \varphi_1 \\ \vdots \\ \varphi_{n-1} \\ \varphi_n \\ \varphi'_n \end{bmatrix}.$$

5. Stability Analysis

In this section, we study the scheme's stability. To check the stability of proposed technique we use Fourier series method. Suppose $Q(p,t)$ is the approximation of Equation (15). We define

$$\zeta^m_j = q^m_j - Q^m_j, \; j = 1, \ldots, n-1, \; m = 0, 1, \ldots, Z \tag{21}$$

and vector

$$\zeta^m = [\zeta^m_1, \zeta^m_2, \ldots, \zeta^m_{n-1}]^T. \tag{22}$$

Equation (21) satisfies Equation (15), the round-off error equation is given as:

$$\begin{aligned} &[rv_1 - l_8 - v_1]\zeta^{m+1}_{j-1} + [rv_2 + l_9 - v_2]\zeta^{m+1}_j + [rv_1 - l_8 - v_1]\zeta^{m+1}_{j+1} - l_7\zeta^{m+1}_{j-2} - l_7\zeta^{m+1}_{j+2} \\ &= r[v_1\zeta^m_{j-1} + v_2\zeta^m_j + v_1\zeta^m_{j+1}] - r\sum_{s=1}^{m} \xi_s[v_1(\zeta^{m-s+1}_{j-1} - \zeta^{m-s}_{j-1}) + v_2(\zeta^{m-s+1}_j - \zeta^{m-s}_j) \\ &\qquad + v_1(\zeta^{m-s+1}_{j+1} - \zeta^{m-s}_{j+1})]. \end{aligned} \tag{23}$$

The IC and BCs become

$$\begin{cases} \zeta^0_j = \varphi(p_j), \; j = 1, 2, \ldots, n, \\ \zeta^m_0 = \Psi_1(t_m), \; \zeta^m_n = \Psi_2(t_m), \; m = 0, 1, \ldots, Z. \end{cases} \tag{24}$$

We define grid function as:

$$\zeta^m = \begin{cases} \zeta^m_j, \;\; p_j - \frac{h}{2} < p \le p_j + \frac{h}{2}, \; j = 1, 2, \ldots, n-1, \\ 0, \;\; a \le p \le a + \frac{h}{2} \;\text{ or }\; b - \frac{h}{2} \le p \le b. \end{cases} \tag{25}$$

The Fourier series representation of ζ^m is given as:

$$\zeta^m(p) = \sum_{n=-\infty}^{\infty} \sigma_m(n) e^{\left(\frac{2\pi inp}{b-a}\right)},\ m = 1, 2, \ldots, Z, \tag{26}$$

where

$$\sigma_m(n) = \frac{1}{b-a} \int_a^b \zeta^m(p) e^{\left(\frac{-2\pi inp}{b-a}\right)} dp. \tag{27}$$

Definition of natural norm yields

$$\begin{aligned} \|\zeta\|_2 &= \left(\sum_{j=1}^{n-1} h \mid \zeta_j^m \mid^2 \right)^{\frac{1}{2}} \\ &= \left[\int_a^{a+\frac{h}{2}} \mid \zeta^m \mid^2 dp + \sum_{j=1}^{Z-1} \int_{p_j-\frac{h}{2}}^{p_j+\frac{h}{2}} \mid \zeta^m \mid^2 dp + \int_{b-\frac{h}{2}}^{b} \mid \zeta^m \mid^2 dp \right]^{\frac{1}{2}} \\ &= \left[\int_a^b \mid \zeta^m \mid^2 dp \right]^{\frac{1}{2}}. \end{aligned}$$

Using the Parseval's identity, we have

$$\int_a^b \mid \zeta^m \mid^2 dp = \sum_{-\infty}^{\infty} \mid \sigma_m(r) \mid^2 .$$

Thus, we obtain

$$\|\zeta^m\|_2^2 = \sum_{-\infty}^{\infty} \mid \sigma_m(r) \mid^2 . \tag{28}$$

Consider, the solution in Fourier series form as:

$$\zeta_k^m = \sigma_m e^{i\theta kh}, \tag{29}$$

where $i = (-1)^{\frac{1}{2}}$ and $\theta = \frac{2\pi m}{b-a}$. Substituting Equation (29) in (23), we achieve

$$\begin{aligned} &[rv_1 - l_8 - v_1]\sigma_{m+1} e^{i\theta(k-1)h} + [rv_2 + l_9 - v_2]\sigma_{m+1} e^{i\theta kh} + [rv_1 - l_8 - v_1]\sigma_{m+1} e^{i\theta(k+1)h} \\ &-l_7\sigma_{m+1}(e^{i\theta(k-2)h} + e^{i\theta(k+2)h}) = r\sigma_m[v_1 e^{i\theta(k-1)h} + v_2 e^{i\theta kh} + v_1 e^{i\theta(k+1)h}] - r\sum_{s=1}^{m} \xi_s[v_1(\sigma_{m-s+1} e^{i\theta(k-1)h} \\ &-\sigma_{m-s} e^{i\theta(k-1)h}) + v_2(\sigma_{m-s+1} e^{i\theta kh} - \sigma_{m-s} e^{i\theta kh}) + v_1(\sigma_{m-s+1} e^{i\theta(k+1)h} - \sigma_{m-s} e^{i\theta(k+1)h})]. \end{aligned} \tag{30}$$

Simplification of the above equation yields

$$\sigma_{m+1} = \frac{1}{u_1}\sigma_m - \frac{1}{u_1}\sum_{s=1}^{m} \xi_s(\zeta_{m-s+1} - \zeta_{m-s}), \tag{31}$$

where

$$u_1 = 1 + \frac{-12 + 2sin^2(\theta\frac{h}{2})(4(4+\varrho) - (4-\varrho)h^2) + 2sin^2(\theta h)(2-\varrho)}{12h^2 r(1 + \frac{\varrho-4}{6})sin^2(\theta\frac{h}{2})}, \tag{32}$$

it is clear that $u_1 \geq 1$ for $\varrho > -2$.

Proposition 1. *Assume that* $\sigma_m,\ m = 1, 2, \ldots, T \times Z$, *satisfy Equation* (31), *we have*

$$\mid \sigma_m \mid \leq \mid \sigma_0 \mid . \tag{33}$$

Proof. To verify inequality (33), we use mathematical induction. Put $m = 0$ in (31), we obtain

$$| \sigma_1 | = \frac{1}{u_1} | \sigma_0 | \leq | \sigma_0 |, \ \frac{1}{u_1} \geq 1.$$

Assume that $| \sigma_m | \leq | \sigma_0 |$ is true for $m = 1, 2, \ldots, T \times Z - 1$. From Equation (31), we obtain

$$\begin{aligned} | \sigma_{m+1} | &\leq \frac{1}{u_1} | \sigma_n | - \frac{1}{u_1} \sum_{s=1}^{m} (\sigma_{m-s+1} - \sigma_{m-s}) \\ &\leq \frac{1}{u_1} | \sigma_0 | - \frac{1}{u_1} \sum_{s=1}^{m} (\sigma_0 - \sigma_0) \\ &\leq | \sigma_0 | . \end{aligned}$$

Hence, inequality (33) is true. □

Theorem 1. *The scheme* (15) *is unconditionally stable.*

Proof. Using above proposition and Equation (28), we acquire

$$\|\zeta^m\|_2 \leq \|\zeta^0\|_2, \ \ m = 0, 1, \ldots, Z,$$

hence, Equation (15) with IC and BCs is unconditionally stable. □

6. Convergence

In this section, convergence of the proposed method is examined that is based on Kadalbajoo and Arora's technique [54].

Theorem 2. *Suppose that* $q(p,t) \in C^4[a,b]$, $\nu \in C^2[a,b]$ *and* $\Theta = [a = p_0, p_1, \ldots, p_n = b]$ *is the equidistant partition of* $[a,b]$ *having length* h. *Consider* $\tilde{Q}(p,t)$ *is a unique spline that interpolates the solution of the propounded problem at knots* $p_0, p_1, \ldots, p_n \in \Theta$, *then there exists a constant* c_j *that does not dependent on* h, *so* $\forall\ t \geq 0$, *we have*

$$\|D^j(q(p,t) - Q(p,t))\|_\infty \leq c_j h^{4-j}, \ \ j = 0, 1, 2. \tag{34}$$

Lemma 2 (see [58])**.** *The ExCBS set* $\{C_{-1}, C_0, \ldots, C_{n+1}\}$ *defined in* (4) *satisfies the following inequality*

$$\sum_{j=-1}^{n+1} | C_j(p, \varrho) | \leq \frac{7}{4}, \qquad 0 \leq p \leq 1. \tag{35}$$

Theorem 3. *Consider the approximation for the exact solution* $q(p,t)$ *is* $Q(p,t)$ *of the time-dependent FPDEs. Further, if* $\nu \in C^2[0,1]$, *then the inequality*

$$\|q(p,t) - Q(p,t)\|_\infty \leq \Phi h^2, \tag{36}$$

exists for every $t \geq 0$, h *is sufficiently small and* Φ *is a positive constant not depending on* h.

Proof. Consider the calculated spline approximation is $\tilde{Q}(p,t)$ to the approximate solution $Q(p,t)$, where $\tilde{Q}(p,t) = \sum_{j=-1}^{n+1} \check{d}_j C_k(p)$. From triangular inequality, we obtain

$$\|q(p,t) - Q(p,t)\|_\infty \leq \|q(p,t) - \tilde{Q}(p,t)\|_\infty + \|\tilde{Q}(p,t) - Q(p,t)\|_\infty. \tag{37}$$

From inequality (34), we have

$$\|D^j(q(p,t)-\tilde{Q}(p,t))\|_\infty \le c_j h^{4-j},\ \ j=0,1,2. \tag{38}$$

Using Equation (37), we achieve

$$\|q(p,t)-Q(p,t)\|_\infty \le c_0 h^4 + \|\tilde{Q}(p,t)-Q(p,t)\|_\infty. \tag{39}$$

The collocation conditions are:

$$Lq(p_j,t) = LQ(p_j,t) = g(p_j,t),\ \ j=0,1,\ldots,n.$$

Let

$$L\tilde{Q}(p,t) = \bar{g}(p_j,t),\ \ j=0,1,\ldots,n.$$

Therefore, the difference equation $L(\tilde{Q}(p_j,t)-Q(p_j,t))$ of the given problem for any time level m is described as

$$\begin{aligned}[rv_1-l_8-v_1]\varsigma_{j-1}^{m+1}+[rv_2+l_9-v_2]\varsigma_j^{m+1}+[rv_1-l_8-v_1]\varsigma_{j+1}^{m+1}-l_7\varsigma_{j-2}^{m+1}-l_7\varsigma_{j+2}^{m+1}\\ = r[v_1\varsigma_{j-1}^m+v_2\varsigma_j^m+v_1\varsigma_{j+1}^m]-r\sum_{s=1}^{m}\xi_s[v_1(\varsigma_{j-1}^{m-s+1}-\varsigma_{j-1}^{m-s})+v_2(\varsigma_j^{m-s+1}-\varsigma_j^{m-s})\\ +v_1(\varsigma_{j+1}^{m-s+1}-\varsigma_{j+1}^{m-s})]+g^{m+1},\end{aligned} \tag{40}$$

for $j=0,n$, we have

$$\begin{aligned}[rv_1-l_1-v_1]\varsigma_{-1}^{m+1}+[rv_2-l_2-v_2]\varsigma_0^{m+1}+[rv_1-l_3-v_1]\varsigma_1^{m+1}-l_4\varsigma_2^{m+1}-l_5\varsigma_3^{m+1}\\ -l_6\varsigma_4^{m+1} = r[v_1\varsigma_{-1}^m+v_2\varsigma_0^m+v_1\varsigma_1^m]-r\sum_{s=1}^{m}\xi_s[v_1(\varsigma_{-1}^{m-s+1}-\varsigma_{-1}^{m-s})+v_2(\varsigma_0^{m-s+1}-\varsigma_0^{m-s})\\ +v_1(\varsigma_1^{m-s+1}-\varsigma_1^{m-s})]+g^{m+1}\end{aligned} \tag{41}$$

and

$$\begin{aligned}[rv_1-l_3-v_1]\varsigma_{n-1}^{m+1}+[rv_2-l_2-v_2]\varsigma_n^{m+1}+[rv_1-l_1-v_1]\varsigma_{n+1}^{m+1}-l_6\varsigma_{n-4}^{m+1}-l_5\varsigma_{n-3}^{m+1}\\ -l_4\varsigma_{n-2}^{m+1} = r[v_1\varsigma_{n-1}^m+v_2\varsigma_n^m+v_1\varsigma_{n+1}^m]-r\sum_{s=1}^{m}\xi_s[v_1(\varsigma_{n-1}^{m-s+1}-\varsigma_{n-1}^{m-s})+v_2(\varsigma_n^{m-s+1}-\varsigma_n^{m-s})\\ +v_1(\varsigma_{n+1}^{m-s+1}-\varsigma_{n+1}^{m-s})]+g^{m+1}.\end{aligned} \tag{42}$$

The BCs for Equations (41) and (42) are

$$v_1\varsigma_{-1}^{m+1}+v_2\varsigma_0^{m+1}+v_1\varsigma_1^{m+1}=0,$$

$$v_1\varsigma_{n-1}^{m+1}+v_2\varsigma_n^{m+1}+v_1\varsigma_{n+1}^{m+1}=0,$$

where

$$\varsigma_j^m = \eta_j^m - \check{d}_j^m,\ \ j=-1,0,1,\ldots,n+1.$$

Using (38), we obtain

$$\kappa_j^m = h^2[g_j^m-\bar{g}_j^m] \le ch^4,\ \ j=0,1,\ldots,n.$$

Define

$$\kappa^m = max\{|\ \kappa_j^m\ |;0\le j\le n\},\ \check{e}_j^m = |\ \varsigma_j^m\ |\ and\ \check{e}^m = max\{|\ \check{e}_j^m\ |;0\le j\le n\}.$$

Put $m=0$, in Equation (40), we obtain

$$[rv_1 - l_8 - v_1]\varsigma_{j-1}^1 + [rv_2 + l_9 - v_2]\varsigma_j^1 + [rv_1 - l_8 - v_1]\varsigma_{j+1}^1 - l_7\varsigma_{j-2}^1 - l_7\varsigma_{j+2}^1 = r[v_1\varsigma_{j-1}^0 + v_2\varsigma_j^0 + v_1\varsigma_{j+1}^0] + g^1,$$

using IC, $\breve{e}^0 = 0$:

$$[rv_2 + l_9 - v_2]\varsigma_j^1 = -[rv_1 - l_8 - v_1][\varsigma_{j-1}^1 + \varsigma_{j+1}^1] + l_7[\varsigma_{j-2}^1 + \varsigma_{j+2}^1] + \frac{1}{h^2}\kappa_j^1,$$

taking absolute values of ς_j^m and κ_j^m, we achieve

$$\breve{e}_j^1 \leq \frac{6ch^4}{h^2r(2+\varrho) + 4\varrho - h^2(2+\varrho) + 16}.$$

Put $m = 0$, in Equations (41) and (42), we acquire

$$[rv_1 - l_1 - v_1]\varsigma_{-1}^1 + [rv_2 + l_2 - v_2]\varsigma_0^1 + [rv_1 - l_3 - v_1]\varsigma_{+1}^1 - l_4\varsigma_2^1 - l_5\varsigma_3^1 - l_6\varsigma_4^1 = r[v_1\varsigma_{-1}^0 + v_2\varsigma_0^0 + v_1\varsigma_1^0] + g^1$$

and

$$[rv_1 - l_3 - v_1]\varsigma_{n-1}^1 + [rv_2 + l_2 - v_2]\varsigma_n^1 + [rv_1 - l_1 - v_1]\varsigma_{n+1}^1 - l_6\varsigma_{n-4}^1 - l_5\varsigma_{n-3}^1 - l_4\varsigma_{n-2}^1 = r[v_1\varsigma_{-1}^0 + v_2\varsigma_0^0 + v_1\varsigma_1^0] + g^1,$$

using IC, $\breve{e}^0 = 0$:

$$[rv_2 + l_2 - v_2]\varsigma_0^1 = -[rv_1 - l_1 - v_1]\varsigma_{-1}^1 - [rv_1 - l_3 - v_1]\varsigma_{+1}^1 + l_4\varsigma_2^1 + l_5\varsigma_3^1 + l_6\varsigma_4^1 + \frac{1}{h^2}\kappa_0^1$$

and

$$[rv_2 + l_2 - v_2]\varsigma_n^1 = -[rv_1 - l_3 - v_1]\varsigma_{n-1}^1 - [rv_1 - l_1 - v_1]\varsigma_{n+1}^1 + l_6\varsigma_{n-4}^1 + l_5\varsigma_{n-3}^1 + l_4\varsigma_{n-2}^1 + \frac{1}{h^2}\kappa_n^1,$$

taking absolute values of ς_0^1 and κ_0^1, we have

$$\breve{e}_0^1 \leq \frac{6ch^4}{h^2r(2+\varrho) - 9\varrho - h^2(2+\varrho) + 42},$$

also for $j = n$

$$\breve{e}_n^1 \leq \frac{6ch^4}{h^2r(2+\varrho) - 9\varrho - h^2(2+\varrho) + 42}.$$

Using BCs, we conclude that

$$\breve{e}_{-1}^1 \leq c_1h^2, \;\; \breve{e}_{n+1}^1 \leq c_1h^2. \tag{43}$$

Hence,

$$\breve{e}^1 \leq c_1h^2, \tag{44}$$

where c_1 is independent of h.

Using induction procedure on m, suppose that $\breve{e}_j^y \leq c_yh^2$ for $y = 1, 2, \ldots, m$.

Let $c = max\{c_y : 0 \leq y \leq m\}$. Then, the Equation (40) becomes

$$\begin{aligned}
&[rv_1 - l_8 - v_1]\varsigma_{j-1}^{m+1} + [rv_2 + l_9 - v_2]\varsigma_j^{m+1} + [rv_1 - l_8 - v_1]\varsigma_{j+1}^{m+1} - l_7\varsigma_{j-2}^{m+1} - l_7\varsigma_{j+2}^{m+1} \\
&= r\xi_0[v_1\varsigma_{j-1}^m + v_2\varsigma_j^m + v_1\varsigma_{j+1}^m] - r[\xi_1(v_1(\varsigma_{j-1}^m - \varsigma_{j-1}^{m-1}) + v_2(\varsigma_j^m - \varsigma_j^{m-1}) + v_1(\varsigma_{j+1}^m - \varsigma_{j+1}^{m-1})) \\
&+\xi_2(v_1(\varsigma_{j-1}^{m-1} - \varsigma_{j-1}^{m-2}) + v_2(\varsigma_j^{m-1} - \varsigma_j^{m-2}) + v_1(\varsigma_{j+1}^{m-1} - \varsigma_{j+1}^{m-2})) + \ldots + \xi_m(v_1(\varsigma_{j-1}^1 - \varsigma_{j-1}^0) \\
&+v_2(\varsigma_j^1 - \varsigma_j^0) + v_1(\varsigma_{j+1}^1 - \varsigma_{j+1}^0))] + g^{m+1},
\end{aligned}$$

taking absolute values of ς_j^m and κ_j^m, we obtain

$$\breve{e}_j^{m+1} \leq \frac{6ch^2}{h^2r(2+\varrho)+4\varrho-h^2(2+\varrho)+16}\left(r\sum_{s=0}^{m}(\xi_s-\xi_{s+1})ch^2+ch^2\right),$$

also from BCs:

$$\breve{e}_j^{m+1} \leq ch^2.$$

Thus, $\forall m$, we have

$$\breve{e}_j^{m+1} \leq ch^2. \tag{45}$$

From above equation and Lemma 2, we have

$$\tilde{Q}(p,t)-Q(p,t)=\sum_{j=-1}^{n+1}(\breve{d}_j(t)-\eta_j(t))C_j(p,\varrho).$$

Taking the norm, we obtain

$$\|q(p,t)-\tilde{Q}(p,t)\|_\infty \leq 1.75ch^2.$$

Using above inequality and Equation (45), we achieve

$$\|q(p,t)-\tilde{Q}(p,t)\|_\infty+\|\tilde{Q}(p,t)-Q(p,t)\|_\infty \leq c_0h^4+1.75ch^2=\Phi h^2,$$

where $\Phi=c_0h^2+1.75c$.

Equation (14) and previous theorem show that the proposed method converges, i.e.,

$$\|q(p,t)-Q(p,t))\|_\infty \leq \Phi h^2+\delta(\triangle t)^{2-\gamma},$$

where Φ and δ are constants. □

7. Numerical Results

Two numerical examples are demonstrated for TFACE to examine the efficiency of proposed scheme. To test the scheme, the error norms L_2, L_∞ and relative error are used. These are defined as:

$$L_2=\sqrt{h\sum_{j=0}^{n}|Q(p_j,t)-q(p_j,t)|^2},\ L_\infty=\max_{0\leq j\leq n}|Q(p_j,t)-q(p_j,t)|$$

and

$$\text{Relative error}=\left|\frac{Q(p_j,t)-q(p_j,t)}{q(p_j,t)}\right|.$$

All the calculations are performed with the help of Mathematica 9.0 software.

Problem 1. *Let the TFACE*

$$\frac{\partial^\gamma q(p,t)}{\partial t^\gamma}-\frac{\partial^2 q(p,t)}{\partial p^2}+(q(p,t))^3-q(p,t)=\nu(p,t),\ \ a\leq p\leq b,\ 0\leq t\leq T,$$

where $\nu(p,t)=(\gamma+1)(p-1)pt\Gamma(1+\gamma)+(p^2-p)^3t^{3+3\gamma}-(p^2-p+2)t^{1+\gamma}$.

We can obtain IC and BCs from the exact solution $(p^2-p)t^{1+\gamma}$. The maximum absolute error is demonstrated in Tables 1 and 2 for different values of p by taking $\gamma=\frac{7}{10}$, $\frac{9}{10}$, $n=100$, $p\in[0,1]$, $\Delta t=\frac{1}{1000}$ and $t=1$. In Table 3, L_2 and L_∞ norms are expounded for $\gamma=\frac{2}{10}$, $\frac{5}{10}$, $\frac{8}{10}$ for different values of t. Figure 1 represents the physical behavior of exact and approximate results against various values of time for $\gamma=\frac{4}{10}$, $n=60$, $\Delta t=\frac{1}{1000}$

and $p \in [-1, 2]$. The 3D graphical representation for exact and numerical solutions when $n = 80$, $t = \frac{2}{10}$, $\gamma = \frac{6}{10}$ and $\Delta t = \frac{1}{1000}$ is shown in Figure 2. True and numerical solutions for distinct values of γ are exhibited in Figure 3. A comparison of three-dimensional graphs for $n = 100$, $t = \frac{2}{10}$, $\gamma = \frac{4}{10}$ and $\Delta t = \frac{1}{100}$ is presented in Figure 4.

Table 1. Absolute error at $t = 1$ whereas $\gamma = \frac{7}{10}$, $\Delta t = \frac{1}{1000}$ and $n = 100$ for Problem 1 using proposed scheme.

$p/t \rightarrow$	$\frac{1}{10}$	$\frac{2}{10}$	$\frac{3}{10}$	$\frac{4}{10}$	$\frac{5}{10}$	$\frac{6}{10}$	$\frac{7}{10}$	$\frac{8}{10}$	$\frac{9}{10}$
$\frac{1}{10}$	7.7669×10^{-7}	6.8604×10^{-7}	6.2886×10^{-7}	6.0350×10^{-7}	6.1561×10^{-7}	6.7886×10^{-7}	8.1346×10^{-7}	1.0454×10^{-6}	1.4058×10^{-6}
$\frac{2}{10}$	1.4691×10^{-6}	1.2984×10^{-6}	1.1911×10^{-6}	1.1453×10^{-6}	1.1731×10^{-6}	1.3017×10^{-6}	1.5715×10^{-6}	2.0338×10^{-6}	2.7504×10^{-6}
$\frac{3}{10}$	2.0109×10^{-6}	1.7783×10^{-6}	1.6327×10^{-6}	1.5735×10^{-6}	1.6189×10^{-6}	1.8089×10^{-6}	2.2017×10^{-6}	2.8714×10^{-6}	3.9063×10^{-6}
$\frac{4}{10}$	2.3548×10^{-6}	2.0833×10^{-6}	1.9139×10^{-6}	1.8477×10^{-6}	1.9075×10^{-6}	2.1424×10^{-6}	2.6234×10^{-6}	3.4402×10^{-6}	4.7002×10^{-6}
$\frac{5}{10}$	2.4726×10^{-6}	2.1878×10^{-6}	2.0105×10^{-6}	1.9421×10^{-6}	2.0074×10^{-6}	2.2589×10^{-6}	2.7720×10^{-6}	3.6424×10^{-6}	4.9841×10^{-6}
$\frac{6}{10}$	2.3548×10^{-6}	2.0833×10^{-6}	1.9139×10^{-6}	1.8477×10^{-6}	1.9075×10^{-6}	2.1424×10^{-6}	2.6234×10^{-6}	3.4402×10^{-6}	4.7002×10^{-6}
$\frac{7}{10}$	2.0109×10^{-6}	1.7783×10^{-6}	1.6327×10^{-6}	1.5735×10^{-6}	1.6189×10^{-6}	1.8089×10^{-6}	2.2017×10^{-6}	2.8714×10^{-6}	3.9063×10^{-6}
$\frac{8}{10}$	1.4691×10^{-6}	1.2984×10^{-6}	1.1911×10^{-6}	1.1453×10^{-6}	1.1731×10^{-6}	1.3017×10^{-6}	1.5715×10^{-6}	2.0338×10^{-6}	2.7504×10^{-6}
$\frac{9}{10}$	7.7669×10^{-7}	6.8604×10^{-7}	6.2886×10^{-7}	6.0350×10^{-7}	6.1561×10^{-7}	6.7886×10^{-7}	8.1346×10^{-7}	1.0454×10^{-6}	1.4057×10^{-6}

Table 2. Absolute error at $t = 1$ whereas $\gamma = \frac{9}{10}$, $\Delta t = \frac{1}{1000}$ and $n = 100$ for Problem 1 using proposed technique.

$p/t \rightarrow$	$\frac{1}{10}$	$\frac{2}{10}$	$\frac{3}{10}$	$\frac{4}{10}$	$\frac{5}{10}$	$\frac{6}{10}$	$\frac{7}{10}$	$\frac{8}{10}$	$\frac{9}{10}$
$\frac{1}{10}$	3.0507×10^{-6}	3.5748×10^{-6}	3.6734×10^{-6}	3.6690×10^{-6}	3.6545×10^{-6}	3.6715×10^{-6}	3.7543×10^{-6}	3.9420×10^{-6}	4.2838×10^{-6}
$\frac{2}{10}$	5.7631×10^{-6}	6.7627×10^{-6}	6.9522×10^{-6}	6.9461×10^{-6}	6.9223×10^{-6}	6.9623×10^{-6}	7.1331×10^{-6}	7.5125×10^{-6}	8.1981×10^{-6}
$\frac{3}{10}$	7.8782×10^{-6}	9.2577×10^{-6}	9.5210×10^{-6}	9.5159×10^{-6}	9.4894×10^{-6}	9.5559×10^{-6}	9.8119×10^{-6}	1.0369×10^{-5}	1.1368×10^{-5}
$\frac{4}{10}$	9.2171×10^{-6}	1.0841×10^{-5}	1.1153×10^{-5}	1.1150×10^{-5}	1.1124×10^{-5}	1.1213×10^{-5}	1.1532×10^{-5}	1.2218×10^{-5}	1.3442×10^{-5}
$\frac{5}{10}$	9.6748×10^{-6}	1.1384×10^{-5}	1.1713×10^{-5}	1.1710×10^{-5}	1.1685×10^{-5}	1.1782×10^{-5}	1.2125×10^{-5}	1.2859×10^{-5}	1.4164×10^{-5}
$\frac{6}{10}$	9.2171×10^{-6}	1.0841×10^{-5}	1.1153×10^{-5}	1.1150×10^{-5}	1.1124×10^{-5}	1.1213×10^{-5}	1.1532×10^{-5}	1.2218×10^{-5}	1.3442×10^{-5}
$\frac{7}{10}$	7.8782×10^{-6}	9.2577×10^{-6}	9.5210×10^{-6}	9.5159×10^{-6}	9.4894×10^{-6}	9.5559×10^{-6}	9.8191×10^{-6}	1.0369×10^{-5}	1.1368×10^{-5}
$\frac{8}{10}$	5.7631×10^{-6}	6.7627×10^{-6}	6.9522×10^{-6}	6.9461×10^{-6}	6.9223×10^{-6}	6.9623×10^{-6}	7.1331×10^{-6}	7.5125×10^{-6}	8.1981×10^{-6}
$\frac{9}{10}$	3.0507×10^{-6}	3.5748×10^{-6}	3.6734×10^{-6}	3.6690×10^{-6}	3.6545×10^{-6}	3.6715×10^{-6}	3.7543×10^{-6}	3.9420×10^{-6}	4.2838×10^{-6}

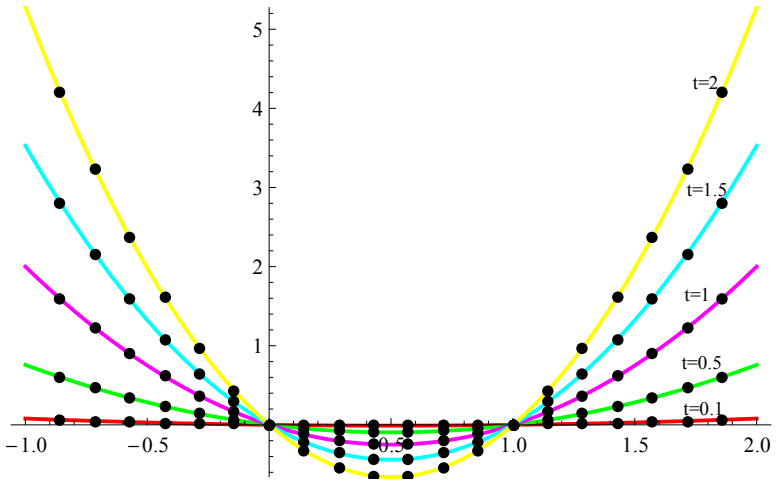

Figure 1. Comparison of exact and numerical solutions for Problem 1, when $n = 60$, $\Delta t = \frac{1}{1000}$, $\gamma = \frac{4}{10}$ and $p \in [-1, 2]$.

Table 3. Error norms at $n = 64$ and $\Delta t = \frac{1}{1000}$ for Problem 1.

t	$\gamma = \frac{2}{10}$		$\gamma = \frac{5}{10}$		$\gamma = \frac{8}{10}$	
	L_2	L_∞	L_2	L_∞	L_2	L_∞
$\frac{2}{10}$	5.3732×10^{-8}	7.7949×10^{-8}	2.5749×10^{-7}	3.6346×10^{-7}	3.6244×10^{-6}	2.1065×10^{-6}
$\frac{4}{10}$	2.8559×10^{-7}	4.1604×10^{-7}	3.1042×10^{-7}	4.4471×10^{-7}	3.3835×10^{-6}	4.7715×10^{-6}
$\frac{6}{10}$	8.1687×10^{-7}	1.1901×10^{-6}	7.2269×10^{-7}	1.0486×10^{-6}	3.4561×10^{-6}	4.8922×10^{-6}
$\frac{8}{10}$	1.7279×10^{-6}	2.5170×10^{-6}	1.7500×10^{-6}	2.5487×10^{-6}	4.2860×10^{-6}	6.1185×10^{-6}
1.0	3.0838×10^{-6}	4.4917×10^{-6}	3.7141×10^{-6}	5.4136×10^{-6}	6.5905×10^{-6}	9.4974×10^{-6}

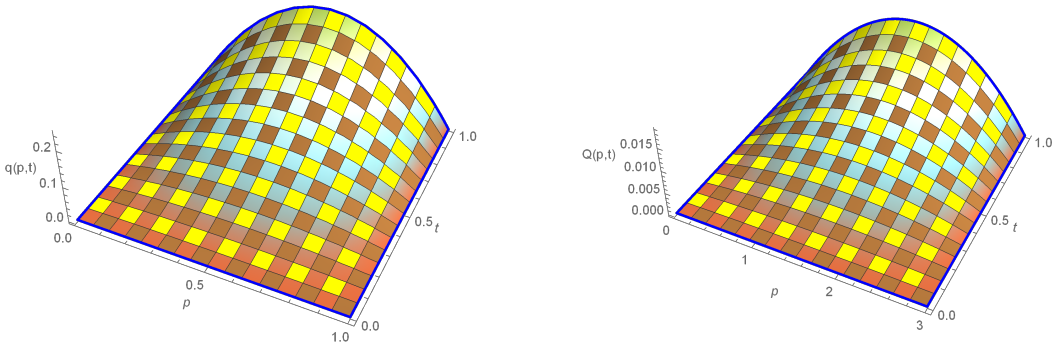

(**a**) (**b**)

Figure 2. Three-dimensional graphs for $n = 80$, $\gamma = \frac{6}{10}$, $t = \frac{2}{10}$ and $\Delta t = \frac{1}{1000}$ of Problem 1. (**a**) Exact solution. (**b**) Numerical solution.

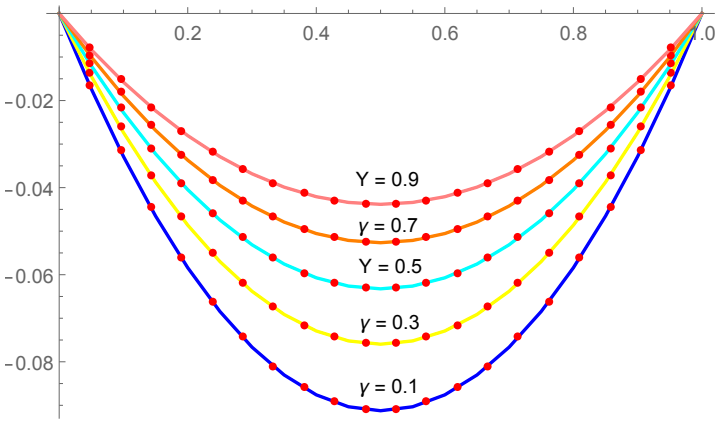

Figure 3. True and approximate solutions for Problem 1, when $n = 20$, $t = \frac{4}{10}$ and $p \in [0, 1]$ for different values of γ.

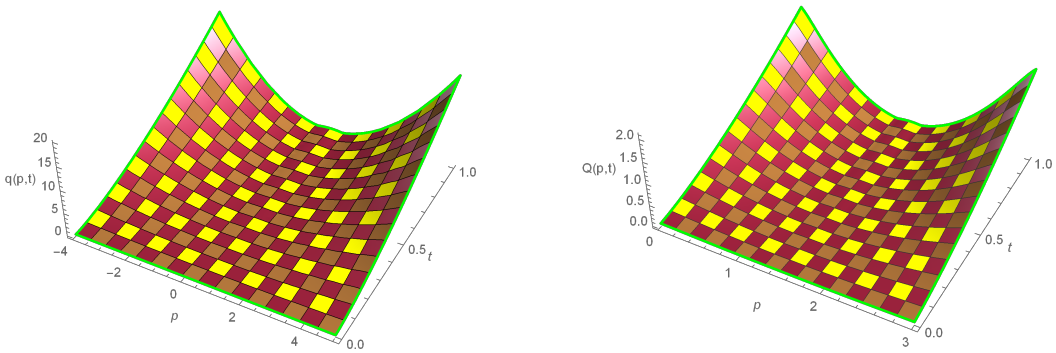

(**a**) (**b**)

Figure 4. 3D graphs for Problem 1, when $n = 100$, $\gamma = \frac{4}{10}$, $t = \frac{2}{10}$ and $p \in [-4, 5]$. (**a**) Exact solution. (**b**) Numerical solution.

Problem 2. *Consider the TFACE*

$$\frac{\partial^{\gamma} q(p,t)}{\partial t^{\gamma}} - \frac{\partial^2 q(p,t)}{\partial p^2} + (q(p,t))^3 - q(p,t) = \nu(p,t), \;\; a \leq p \leq b, \; 0 \leq t \leq T.$$

The source term $\nu(p,t)$ *is given as* $\nu(p,t) = p(p^2-1)^3 p t^{2-\gamma} E_{1,3-\gamma}(t) + 6(7p^4 - 10p^2 + 3)pt^2 E_{1,3}(t) + \frac{1}{2} q(p,t)[q(p,t)-1][2q(p,t)-1]$, *where* $E_{\varepsilon,\upsilon}(\omega)$ *is the Mittag–Leffler function and is defined as:*

$$E_{\varepsilon,\upsilon}(\omega) = \sum_{k=0}^{\infty} \frac{\omega^k}{\Gamma(\varepsilon k + \gamma)}.$$

We can derive IC and BCs from the exact solution $p(1-p^2)t^2 E_{1,3}(t)$. Table 4 represents contrast of the absolute error of proposed scheme with RCBS [59] for $\gamma = \frac{5}{10}$, $n = 10$, $t = \frac{1}{10}$ and $p \in [0,1]$. L_2 norm is demonstrated in Table 5 for distinct values of γ and t for $n = 16$ and $p \in [-1,1]$. The exact and computational solutions are presented graphically in Figure 5 for $n = 100$, $\Delta t = \frac{1}{1000}$, $\gamma = \frac{6}{10}$ and $p \in [-1,1]$. Three-dimensional plot of exact and numerical solutions is shown in Figure 6.

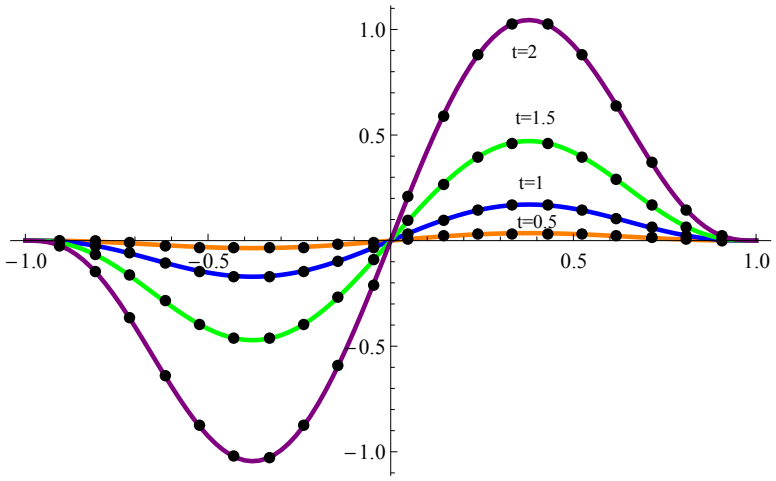

Figure 5. True and numerical solutions for Problem 2 whereas $n = 100$, $\gamma = \frac{6}{10}$ and $p \in [-1,1]$.

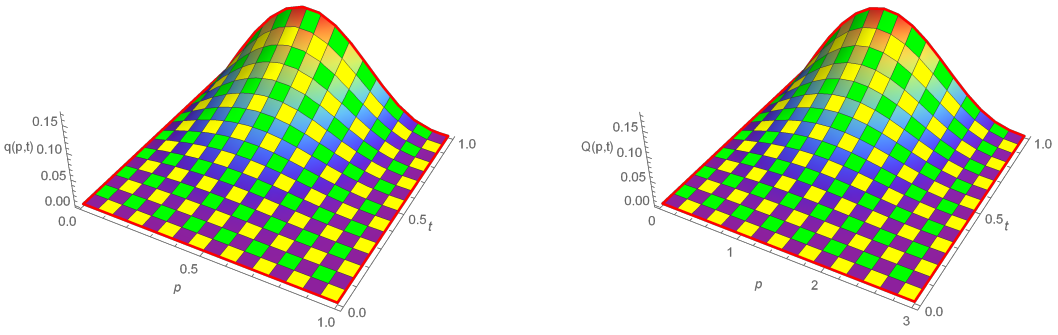

(**a**) (**b**)

Figure 6. 3D representation of Problem 2, when $n = 16$, $\gamma = \frac{8}{10}$, $\Delta t = \frac{1}{1000}$, $t = 1$ and $p \in [0,1]$. (**a**) Exact solution. (**b**) Numerical solution.

Table 4. Absolute error at $t = \frac{1}{10}$ with $\gamma = \frac{5}{10}$, $n = 10$, $\Delta t = \frac{1}{1000}$ and $p \in [0, 1]$ for Problem 2.

p	Approximate Solution			Error		
	Exact Solution	RCBS [59]	Proposed Method	RCBS [59]	Proposed Method	Relative Error
$\frac{1}{10}$	0.0005017	0.0005368	0.0005305	3.511×10^{-5}	2.884×10^{-5}	0.0574846
$\frac{2}{10}$	0.0009149	0.0009807	0.0009686	6.575×10^{-5}	5.364×10^{-5}	0.0586294
$\frac{3}{10}$	0.0011690	0.0012574	0.0012401	8.838×10^{-5}	7.119×10^{-5}	0.0608982
$\frac{4}{10}$	0.0012259	0.0013269	0.0013054	1.010×10^{-4}	7.949×10^{-5}	0.0648422
$\frac{5}{10}$	0.0010907	0.0011941	0.0011691	1.034×10^{-4}	7.838×10^{-5}	0.0718621
$\frac{6}{10}$	0.0008133	0.0009103	0.0008824	9.700×10^{-5}	6.916×10^{-5}	0.0850363
$\frac{7}{10}$	0.0004801	0.0005638	0.0005344	8.364×10^{-5}	5.429×10^{-5}	0.1130806
$\frac{8}{10}$	0.0001930	0.0002574	0.0002295	6.448×10^{-5}	3.657×10^{-5}	0.1894818
$\frac{9}{10}$	0.0000319	0.0000702	0.0000501	3.827×10^{-5}	1.819×10^{-5}	0.5702194

Table 5. L_2 norm for Problem 2 whereas $n = 16$, $\Delta t = \frac{1}{100}$ and $p \in [-1, 1]$.

t	L_2 Error Norm			
	$\gamma = \frac{2}{10}$	$\gamma = \frac{4}{10}$	$\gamma = \frac{6}{10}$	$\gamma = \frac{8}{10}$
$\frac{2}{10}$	4.2131×10^{-4}	3.8615×10^{-4}	3.4429×10^{-4}	3.0779×10^{-4}
$\frac{4}{10}$	1.8453×10^{-3}	1.7443×10^{-3}	1.6251×10^{-3}	1.5002×10^{-3}
$\frac{6}{10}$	4.5702×10^{-3}	4.3721×10^{-3}	4.1522×10^{-3}	3.9264×10^{-3}
$\frac{8}{10}$	9.2039×10^{-3}	8.8084×10^{-3}	8.4023×10^{-3}	8.0129×10^{-3}
1.0	1.7218×10^{-2}	1.6323×10^{-2}	1.5449×10^{-2}	1.4654×10^{-2}

8. Conclusions

In this paper, the TFACE was solved by employing new ExCBS functions and a fully implicit finite difference scheme. The proposed technique was inspected, which proved the scheme is unconditionally stable. The order of convergence that we have calculated is $\Phi h^2 + \delta(\triangle t)^{2-\gamma}$. This scheme was tested with two different problems and results proved the accuracy of this technique. In the future, the ExCBS approach may be used for solving variable order-fractional, space-fractional and higher dimensional FPDEs. Furthermore, it is incredibly helpful for numerically solving various FPDEs with other fractional operators.

Author Contributions: Conceptualization, R.P.A. and M.F.; Data curation, M.S.; Funding acquisition, N.C. and M.A.; Investigation, P.O.M., R.P.A., M.F. and M.A.; Methodology, P.O.M.; Project administration, M.S.; Software, N.C. and M.A.; Supervision, M.A.; Validation, M.S.; Visualization, M.A. and M.F.; Writing—original draft, P.O.M. and R.P.A.; Writing—review and editing, N.C. All of the authors read and approved the final manuscript. All authors have read and agreed to the published version of the manuscript.

Funding: This research received no external funding.

Data Availability Statement: No data were used for the research described in the article.

Acknowledgments: Researchers Supporting Project number (RSP2024R153), King Saud University, Riyadh, Saudi Arabia.

Conflicts of Interest: The authors declare that they have no known competing financial interests or personal relationships that could have appeared to influence the work reported in this paper.

References

1. Kilbas, A.A.; Srivastava, H.M.; Trujillo, J.J. *Thoery and Applications of Fractional Differential Equations*; Elsevier: San Diego, CA, USA, 2006.
2. Machado, J.A.T. A probabilistic interpretationof the fractional oredr differentiation. *Fract. Calc. Appl. Anal.* **2003**, *6*, 73–80.
3. Yousaf, M.Z.; Srivastava, H.M.; Abbas, M.; Nazir, T.; Mohammed, P.O.; Vivas-Cortez, M.; Chorfi, N. A Novel Quintic B-Spline Technique for Numerical Solutions of the Fourth-Order Singular Singularly-Perturbed Problems. *Symmetry* **2023**, *15*, 1929. [CrossRef]

4. Han, X. Piecewise quartic polynomial curves with a local shape parameter. *J. Comput. Appl. Math.* **2006**, *195*, 34–45. [CrossRef]
5. Tariq, H.; Akram, G. New approach for exact solutions of time fractional Cahn-Allen equation and time fractional Phi-4 equation. *Phys. A Stat. Mech. Appl.* **2017**, *473*, 352–362. [CrossRef]
6. Mohammed, P.O.; Machado, J.A.T.; Guirao, J.L.G.; Agarwal, R.P. Adomian decomposition and fractional power series solution of a class of nonlinear fractional differential equations. *Mathematics* **2021**, *9*, 1070. [CrossRef]
7. Ehsan, H.; Abbas, M.; Nazir, T.; Mohammed, P.O.; Chorfi, N.; Baleanu, D. Efficient analytical algorithms to study Fokas dynamical models involving M-truncated derivative. *Qual. Theory Dyn. Syst.* **2024**, *23*, 49. [CrossRef]
8. Lu, B. The first integral method for some time fractional differential equations. *J. Math. Anal. Appl.* **2012**, *395*, 684–693. [CrossRef]
9. He, J.H.; Wu, X.H. Exp-function method for nonlinear wave equations. *Chaos Solitons Fractals* **2006**, *30*, 700–708. [CrossRef]
10. Gepreel, K.A.; Omran, S. Exact solutions for nonlinear partial fractional differential equations. *Chin. Phys. B* 2012, *21*, 110204. [CrossRef]
11. Liu, W.; Chen, K. The functional variable method for finding exact solutions of some non-linear time-fractional differential equations. *Pramana* **2013**, *81*, 377–384. [CrossRef]
12. Bulut, H.; Baskonus, H.M.; Pandir, Y. The modified trial equation method for fractional wave equation and time fractional generalized Burgers equation. *Abstr. Appl. Anal.* **2013**, *2013*, 636802. [CrossRef]
13. Zheng, B.; Wen, C. Exact solutions for fractional partial differential equations by new fractional sub-equation method. *Adv. Differ. Equ.* **2013**, *2013*, 19. [CrossRef]
14. Taghizadeh, N.; Mirzazadeh, M.; Rahimian, M.; Akbari, M. Application of the simplest equation method to sometime-fractional partial differential equations. *Ain Shams Eng. J.* **2013**, *4*, 897–902. [CrossRef]
15. Sahoo, S.; Ray, S.S. New solitary wave solutions of time-fractional coupled Jaulent-Miodek equation by using two reliable methods. *Nonlinear Dyn.* **2016**, *85*, 1167–1176. [CrossRef]
16. Tariq, H.; Akram, G. New traveling wave exact and approximate solutions for the nonlinear Cahn-Allen equation evolution of a nonconserved quantity. *Nonlinear Dyn.* **2013**, *88*, 581–594. [CrossRef]
17. Prüss, J.; Wilke, M. Maximal Lp-regularity and long-time behaviour of the non-isothermal Cahn-Hilliard equation with dynamic boundary conditions. In *Partial Differential Equations and Functions Analysis*; Birkhauser: Basel, Switzerland, 2006; pp. 209–236.
18. Appadu, A.R.; Djoko, J.K.; Gidey, H.H. A priori analysis of multilevel finite volume approximation of 1D convective Cahn-Hilliard equation. *Afr. Mat.* **2017**, *28*, 1193–1233. [CrossRef]
19. Tijani, Y.O., Appadu, A.R. Unconditionally positive NSFD and classical finite difference schemes for biofilm formation on medical implant using Allen-Cahn equation. *Demonstr. Math.* **2022**, *55*, 40–60. [CrossRef]
20. Allen, S.M., & Cahn, J.W. A microscopic theory for antiphase boundary motion and its application to antiphase domain coarsening. *Acta Metall.* **1979**, *27*, 1085–1095.
21. Liu, C.; Shen, J. A phase field model for the mixture of two incompressible fluids and its approximation by a Fourier-spectral method. *Phys. D Nonlinear Phenom.* **2003**, *179*, 211–228. [CrossRef]
22. Yue, P.; Zhou, C.; Feng, J.J.; Ollivier-Gooch, C.F.; Hu, H.H. Phase-field simulations of interfacial dynamics in viscoelastic fluids using finite elements with adaptive meshing. *J. Comput. Phys.* **2006**, *219*, 47–67. [CrossRef]
23. Jan, A.; Srivastava, H.M.; Khan, A.; Mohammed, P.O.; Jan, R.; Hamed, Y.S. In Vivo HIV Dynamics, Modeling the Interaction of HIV and Immune System via Non-Integer Derivatives. *Fractal Fract.* **2023**, *7*, 361. [CrossRef]
24. Li, Z.; Liang, Z.; Yan, Y. High-order numerical methods for solving time fractional partial differential equations. *J. Sci. Comput.* **2016**, *71*, 785–803. [CrossRef]
25. Hamed, M.A.; Nepomnyashchy, A.A. Domain coarsening in a subdiffusive Allen-Cahn equation. *Phys. D Nonlinear Phenom.* **2015**, *308*, 52–58. [CrossRef]
26. Güner, O.; Bekir, A.; Cevikel, A.C. A variety of exact solutions for the time fractional Cahn-Allen equation. *Eur. Phys. J. Plus* **2015**, *130*, 146. [CrossRef]
27. Zhai, S.; Weng, Z.; Feng, X. Fast explicit operator splitting method and time-step adaptivity for fractional non-local Allen-Cahn model. *Appl. Math. Model.* **2016**, *40*, 1315–1324. [CrossRef]
28. Akagi, G.; Schimperna, G.; Segatti, A. Fractional Cahn-Hilliard, Allen-Cahn and porous medium equations. *J. Differ. Equ.* **2016**, *261*, 2935–2985. [CrossRef]
29. Hou, T.; Tang, T.; Yang, J. Numerical analysis of fully discretized Crank-Nicolson scheme for fractional-in-space Allen-Cahn equations. *J. Sci. Comput.* **2017**, *72*, 1214–1231. [CrossRef]
30. Li, Z.; Wang, H.; Yang, D. A space-time fractional phase-field model with tunable sharpness and decay behavior and its efficient numerical simulation. *J. Comput. Phys.* **2017**, *347*, 20–30. [CrossRef]
31. Hosseini, K.; Bekir, A.; Ansari, R. New exact solutions of the conformable time-fractional Cahn-Allen and Cahn-Hilliard equations using the modified Kudryashov method. *Opt. Int. J. Light Electron Opt.* **2017**, *132*, 203–209. [CrossRef]
32. Sakar, M.G.; Saldir, O.; Erdogan, F. An iterative approximation for time-fractional Cahn-Allen equation with reproducing kernel method. *Comput. Appl. Math.* **2018**, *37*, 5951–5964. [CrossRef]
33. Liu, H.; Cheng, A.; Wang, H.; Zhao, J. Time-fractional Allen-Cahn and Cahn-Hilliard phase-field models and their numerical investigation. *Comput. Math. Appl.* **2018**, *76*, 1876–1892. [CrossRef]
34. Yin, B.; Liu, Y.; Li, H.; He, S. Fast algorithm based on TT-M FE system for space fractional Allen-Cahn equations with smooth and non-smooth solutions. *J. Comput. Phys.* **2019**, *379*, 351–372. [CrossRef]

35. Esen, A.; Yagmurlu, N.M.; Tasbozan, O. Approximate analytical solution to time fractional damped Burger and Cahn-Allen equations. *Appl. Math. Inf. Sci.* **2013**, *7*, 1951–1956. [CrossRef]
36. Inc, M.; Yusuf, A.; Aliyu, A.I.; Baleanu, D. Time-fractional Cahn-Allen and time-fractional Klein-Gordon equations: Lie symmetry analysis, explicit solutions and convergence symmetry analysis, explicit solutions and convergence analysis. *Phys. A Stat. Mech. Appl.* **2018**, *493*, 94–106. [CrossRef]
37. Shafiq, M.; Abdullah, F.A.; Abbas, M.; Alzaidi, A.S.M.; Riaz, M.B. Memory effect analysis using piecewise cubic B-spline of time fractional diffusion equation. *Fractals* **2022**, *30*, 2240270. [CrossRef]
38. Shafiq, M.; Abbas, M.; Abdullah, F.A.; Majeed, A.; Abdeljawad, T.; Alqudah, M.A. Numerical solutions of time fractional Burgers' equation involving Atangana-Baleanu derivative via cubic B-spline functions. *Results Phys.* **2022**, *34*, 105244. [CrossRef]
39. Shafiq, M.; Abbas, M.; Abualnaja, K.M.; Huntul, M.J.; Majeed, A.; Nazir, T. An efficient technique based on cubic B-spline functions for solving time-fractional advection diffusion equation involving Atangana-Baleanu derivative. *Eng. Comput.* **2022**, *38*, 901–917. [CrossRef]
40. Khalid, N.; Abbas, M.; Iqbal, M.K.; Baleanu, D. A numerical algorithm based on Modified extended B-spline functions for solving time-fractional diffusion wave equation involving reaction and damping terms. *Adv. Differ. Equ.* **2019**, *2019*, 378. [CrossRef]
41. Akgül, A.; Karatas Akgül, E. A novel method for solutions of fourth-order fractional boundary value problems. *Fractal Fract.* **2019**, *3*, 33. [CrossRef]
42. Tayebi, S.; Momani, S.; Arqub, O.A. The cubic B-spline interpolation method for numerical point solutions of conformable boundary value problems. *Alex. Eng. J.* **2022**, *61*, 1519–1528. [CrossRef]
43. Appadu, A.R.; Kelil, A.S. Some finite difference methods for solving linear fractional KdV equation. *Front. Appl. Math. Stat.* **2023**, *9*, 1261270. [CrossRef]
44. Atangana, A.; Gómez-Aguilar, J.F. Numerical approximation of Riemann-Liouville definition of fractional derivative from Riemann-Liouville to Atangana-Baleanu. *Numer. Methods Partial Differ. Equ.* **2018**, *34*, 1502–1523. [CrossRef]
45. Akgül, E.K. Solutions of the linear and non-linear differential equations within the generalized fractional derivatives. *Chaos Interdiscip. J. Nonlinear Sci.* **2019**, *29*, 023108. [CrossRef] [PubMed]
46. Mittal, R.C.; Jain, R.K. Redefined cubic B-splines collocation method for solving convection-diffusion equations. *Appl. Math. Model.* **2012**, *36*, 5555–5573. [CrossRef]
47. Rashidinia, J.; Sharifi, S. Numerical solution of hyperbolic telegraph equation by cubic B-spline collocation method. *Appl. Math. Comput.* **2012**, *281*, 28–38.
48. Liu, F.; Zhuang, P.; Anh, V. Stablity and convergence of difference methods for space-time fractional advection-diffusion equation. *Appl. Math. Comput.* **2007**, *191*, 12–20. [CrossRef]
49. Diethelm, K.; Freed, A.D. *On Solution of Nonlinear Fractional Order Differential Equations Used in Modeling of Viscoplasticity*; Springer: Berlin/Heidelberg, Germany, 1999; pp. 217–224.
50. Sayevand, K.; Yazdani, A.; Arjang, F. Cubic B-spline collocation method and its application for anomalous fractional diffusion equations in transport dynamic systems. *J. Vib. Control* **2016**, *22*, 2173–2186. [CrossRef]
51. Akram, G.; Tariq, H. Quintic Spline collocaion method for fractional boundary value problem. *J. Assoc. Arab Univ. Basic Appl. Sci.* **2017**, *23*, 57–65.
52. Tasbozan, O.; Esen, A.; Ucar, Y.; Yagmurlu, N.M. A numerical solution to fractional diffusion equation for force free case. *Abstr. Appl. Anal.* **1999**, **2013**, 187383. [CrossRef]
53. Boyce, W.E.; DiPrima, R.C.; Meade, D.B. *Elementary Differential Equations and Boundary Value Problems*, 9th ed.; Wiley: New York, NY, USA, 1992.
54. Kadalbajoo, M.K.; Arora, P. B-spline collocation method for the singular-perturbation problem using artificial viscosity. *Comput. Math. Appl.* **2009**, *57*, 650–663. [CrossRef]
55. de Boor, C. On the convergence of odd-degree spline interpolation. *J. Approx. Theory* **1968**, *1*, 452–463. [CrossRef]
56. Hall, C.A. On error bounds for spline interpolation. *J. Approx. Theory* **1968**, *1*, 209–218. [CrossRef]
57. Srivastava, H.M.; Mohammed, P.O.; Guirao, J.L.G.; Hamed, Y.S. Some higher-degree Lacunary fractional splines in the approximation of fractional differential equations. *Symmetry* **2021**, *13*, 422. [CrossRef]
58. Akram, T.; Abbas, M.; Riaz, M.B.; Ismail, A.I.; Ali, N.M. Development and analysis of new approximation of extended cubic B-spline to the non-linear time fractional Klein-Gorden equation. *Fractals* **2020**, *28*, 2040039. [CrossRef]
59. Khalid, N.; Abbas, M.; Iqbal, M.K.; Baleanu, D. A numerical investigation of Caputo time fractional Allen-Cahn equation using redefined cubic B-spline functions. *Adv. Differ. Equ.* **2020**, *2020*, 158. [CrossRef]